UCLA Intermediate Energy Physics and Relativistic Heavy Ion Group

Proposal

Development of new calorimetric technology for eRHIC

H. Huang, C. Whitten, S. Trentalange, O. Tsai
8/1/2009

UCLA Intermediate Energy Physics and Relativistic Heavy Ion group is interested in detector R&D for the planned eRHIC Collider. We are proposing the development of a new generic technology based on tungsten power and fiber readout to construct sampling electromagnetic and hadronic calorimeters for eRHIC detectors. The proposed technique aims at building very compact and fine grained devices with good energy resolution, hermeticity, homogeneity, timing and position resolution; all of which are desired properties for eRHIC detectors. The generic technology we are proposing to develop is very simple, cost effective and flexible enough for optimization within a particular eRHIC detector design. To our knowledge, this technology has not been used in any previous experiment at any scale - thus an R&D program is required.

1. Introduction.

First, let us give a brief description of the technology we would like to use. We propose to build sampling calorimeters with active elements consisting of fibers. The fibers can be scintillating, quartz, non-scintillating optical fibers or any combination of these depending on the device being built. A combination of different fibers as active elements in the detectors can be selectively used to read out scintillation and/or Cherenkov light produced by showering particles. As the absorber (radiator) we will use tungsten powder for all devices being proposed for construction. It will be shown below that the utilization of tungsten powder as an absorber opens unique ways to construct fiber calorimeters. Common problems that were encountered in previous fiber calorimeters can be potentially eliminated or reduced with our technique. Fig. 1 presents cross sectional snapshots of a typical fiber calorimeter used in the past (H1) and of the prototype discussed in this proposal.

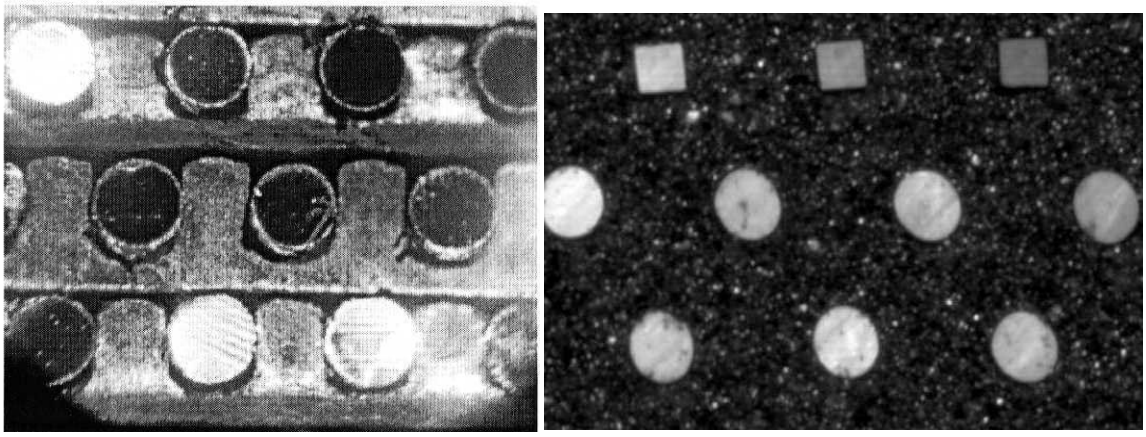

Fig. 1. Fiber/absorber structure of typical ScFi calorimeters (H1 calorimeter) (left); fibers 0.5 mm in diameter, fiber spacing 0.9 mm. (right) Scan of cross section of a second UCLA mechanical prototype made of tungsten powder (square fibers 0.25 mm x 0.25mm, round fiber 0.33 mm, fiber spacing 0.88 mm).

One can ask the question: Why revert to a technique (fiber calorimeters) which was practically abandoned sometime in the mid-1990s, and why is fiber calorimetery of interest to eRHIC? To answer these questions, we would like to refer to a section from the CERN-95-02 Yellow Report "Scintillating-fiber Calorimetry" [1].

"11. Conclusions

Since the moment when fiber calorimeters were first introduced, less then ten years ago, they have rapidly gained a reputation as one of the most attractive detectors available for modern particle physics experiments. This reputation is due to a combination of the following factors:

1. *Fiber calorimeters are among the fastest particle detectors available today. Given the extremely high luminosities, and the correspondingly small time intervals between events, needed to extract envisaged new physics phenomena, this is an important future.*
2. *The excellent resolution in energy and position measurements that can be achieved with a very compact instrument is a property characteristic of fiber calorimeters. As pointed out in section 10.4 this resolution is achieved through very frequent shower sampling and in this way, e.m. energy resolutions of the order of 6%/√E can be achieved with sampling fractions as low as 10% (fig. 104). Depending on the absorber material that is used, the effective density of such a detector will be in the range of 5-10 g/cm, with an effective radiation length of 1 cm or less and Molière radius of 2 cm or less. Given the high cost of radial space in 4π experiments and the high particle density, which makes pencil-like showers very desirable, these are invaluable detector properties.*
3. *The fiber structure of the active calorimeter material has solved the hermeticity problem inherent to all scintillator-based calorimeters used in the past. Since the fibers both generate the light and transport it to the outside world, no separate wavelength-shifting devices, with corresponding non-hermeticity introduced by these, are needed. …*
4. *The high light yield makes it possible to achieve energy resolution compatible with the once obtained with the homogeneous calorimeters. The KLOE Collaboration (section 8.3) found that the contribution of the photoelectron statistics to the energy resolution of their calorimeter was only 2%/√E. The 1500 photoelectrons per GeV found by RD1 for their calorimeter [67], which had a sampling fraction of less then 5% for e.m. showers, limit the contribution of photon statistics to the resolution to only 2.6%/√E. Combined with the extraordinarily low noise levels achieved with the PM readout, this high light yield makes dynamic range of fiber calorimeters very large (at least 6 orders of magnitude). As a result, small energy deposits, for example in the tails of hadronic showers or from traversing muons, can be accurately measured.*
5. *Last but not least, fibre calorimeters are cheap devices. Depending on the complexity of the readout, high-resolution e.m. fibre calorimeters are up to an order of magnitude cheaper than crystal calorimeters (BGO, BaF_2, CeF_3, $PbWO_4$, HfF_4, etc.).*

   Some of the advantages listed above are especially important for the detection of electromagnetic showers. For example, the energy resolution of hadron calorimeters is also determined by factors other than sampling fluctuations and, therefore, does not benefit from choosing fibers to the same extent as e.m. calorimeters. Also, hermeticity requirements are

usually less stringent in the hadronic section of the calorimeters system. Obviously, as illustrated by SPACAL, one can also make excellent hadron calorimeters with the scintillating fibers as active elements, but the advantages over other techniques are somewhat less striking that in the case of e.m. shower detectors."

Although development of new EM calorimeters based on fiber technology was indeed halted, the development of fiber *hadronic* calorimeters has proceeded successfully over the past few years. One of the authors of the report cited above (R.Wigmans) essentially contradicted the last sentence in his own report with the successful R&D DREAM (Dual-REAdout Module) project which, in our opinion, was a cornerstone for the 4'th concept detector for the ILC. The term "Dual-REAdout" refers to readout of scintillation and Cherenkov light at the same time from different fibers (sc. and non-sc.) in a hadron calorimeter. This allows the measurement of the electromagnetic fraction in the hadronic shower on an event-by-event basis. The authors of the DREAM project argue that with this approach the theoretical resolution limit of ~15%/√E for hadronic showers seems to be within reach [2]. The results of the DREAM project were presented at the XIth International Conference on Calorimetry in High Energy Physics (Peruga, Italy, 2004) and were considered by many to be the most significant new development in calorimetry in recent history.

To summarize this section we present two tables with the available EM and hadronic resolution data for fiber calorimeters. The following expressions were used for energy resolutions:

$$\frac{\sigma}{E} = \frac{a}{\sqrt{E}} + c \qquad (1)$$

$$\left(\frac{\sigma}{E}\right)^2 = \left(\frac{a}{\sqrt{E}}\right)^2 + (c)^2 \qquad (2)$$

Detector	Composition	Energy Range (GeV)	a,c eq. (1)	a,c eq.(2)	Comments
Burmeister *et al.*	Pb 1:1	0.04-1	9.8, -		Fibers ø = 1mm, Ribbons ⊥ to the beam.
JETSET	Pb 35:50	0.3-1.5	6.3, -		ø = 1mm, glue 15%
SPACAL	Pb 4:1	5-150	12.9,1.23	15.7, 1.99	ø = 1mm
RD1	Pb 4:1	10-150	9.2, 0.63	10.9, 1.11	ø = 0.5mm
RD1	Pb 1.8:1	10-150	8.0, 0.35	8.9, 0.72	ø = 1mm
RD25	Pb 4:1	2-50	15.0, 0.5	16.0, 1.4	ø = 1mm
RD25	Pb 4:1	2-80	14.4, 0.17	14.7, 0.68	ø = 1mm
LEP-5	Alloy 4:1	2-8	16.0, 1.6		ø = 1mm
KLOE	Pb 35:50	0.02-0.08	4.8, -		ø = 1mm, glue 15%, fibers ⊥ to the beam.
CHORUS	Pb 4:1	2.5-10	13.9, 0.1	14.1, 0.7	ø = 1mm, fibers ⊥ to the beam.
H1	Pb 2.27:1	2-60		7.1, 1	ø = 0.5mm

Table 1. Electromagnetic resolution of fiber calorimeters. Data taken from [1] and [3].

The total hadronic resolution of the two best calorimeters (approximately compensated) and the various factors contributing to it are listed in the table below (where σ_p, σ_s, σ_i are the fluctuations in the number of signal quanta, sampling fluctuation and intrinsic fluctuations, respectively.)

	ZEUS ^{238}U	ZEUS Pb	SPACAL
σ_p	6%/√E	10%/√E	5%/√E
σ_s	31%/√E	42%/√E	27%/√E
σ_i	19%/√E	11%/√E	11%√E
σ_h	37%/√E	44%/√E	30%/√E

Table 2. Hadronic energy resolution of different calorimeters. Data taken from [4,5,6,7]

In all three detectors, the hadronic resolution is dominated by sampling fluctuations. This is a direct consequence of compensation (*e/h =1),* which requires small sampling fractions, for example, 2.3% for lead/plastic detectors and 5.1% for uranium/plastic devices. In the hadronic section of our proposal, we will show that with our technique, it is quite possible to reduce the sampling fluctuations in a compensating hadron calorimeter by increasing the sampling frequency to a level which was considered impractical for traditional methods of construction of fiber calorimeters.

The rest of the proposal is organized as follows. First, in Figure 2 we present a possible road map for proposed the R&D. In the electromagnetic section (Section 2) we will briefly summarize past developments in fiber calorimetry technology, including our own results. In the hadronic section (Section 3) we will discuss both compensated and DREAM type applications with our technique.

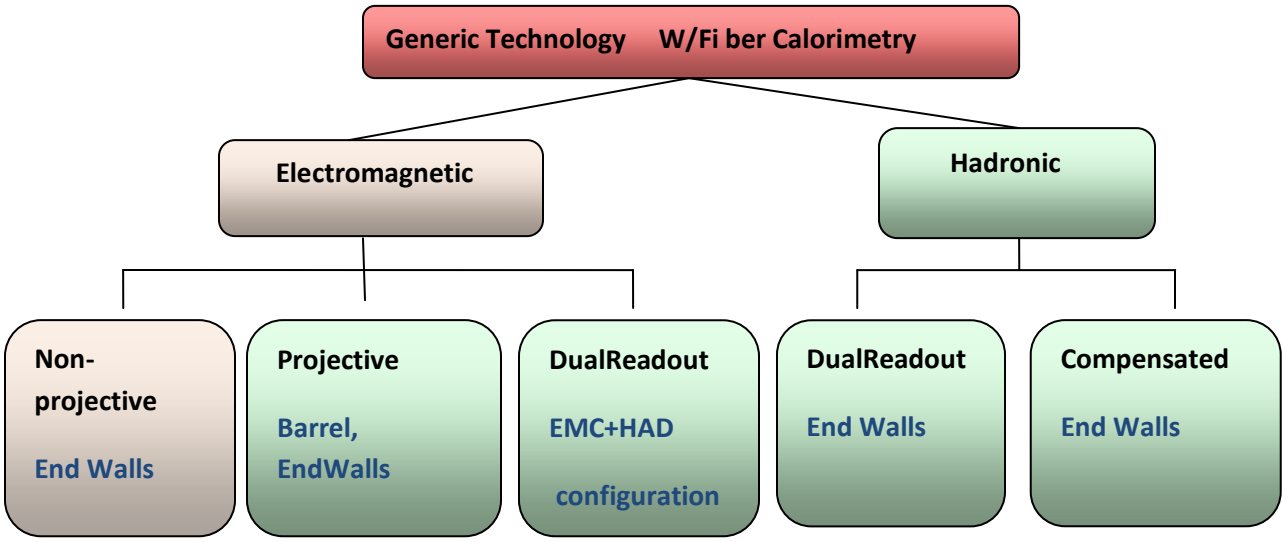

Fig 2. Possible R&D directions and applications for eRHIC detector(s).

The presentation in Figure 2 reflects both possible R&D directions and applications at eRHIC. For example, the most basic and simplest would be an electromagnetic calorimeter with non-projective geometry which may be used in the end walls. Successful tests of a prototype build with such technology would be a proof of principle. All other directions are interesting topics on their own, but they require an initial proof of principle. More detailed discussions will be given below.

2. Electromagnetic fiber calorimeters R&D .

The precision of sampling calorimetric measurements is determined and limited by fluctuations. Among the many factors that play a role are photo-statistics, leakage fluctuations, instrument effects like internal non-uniformities, and the always dominant sampling fluctuations in reasonably designed detectors. Sampling fluctuations are determined by the amount of active material(s) in the detector (sampling fraction) and the sampling frequency (thickness of active layers). In calorimeters with non-gaseous active media energy, the resolution is well described by [8]:

$$\frac{\sigma}{E} = \frac{2.7\%}{\sqrt{E}} * \sqrt{\frac{d}{Fs}} \qquad (3)$$

where *d* is the thickness of the active elements (e.g., diameter of the fibers in mm) and F_S is the sampling fraction for mips. The use of fibers as active material is mainly motivated by the frequent shower sampling achievable in this way. In order to understand the importance of sampling frequency on the energy resolution it is important to realize that the energy of a showering photon or electron is primarily deposited in the absorber material by a large number of very soft secondary electrons. As discussed in [9] these electrons, with energies far below the critical energy, have a range that is typically much smaller than the distance between subsequent sampling layers. This is particularly true for devices which have a high Z absorber and low Z for the active layers. Sampling fluctuations can be interpreted as the statistical fluctuations in the number of electrons that contribute to the calorimeter signal. This number can be increased by increasing the total surface of the boundary between the active and passive material in the calorimeter volume. For fiber calorimeters this is done by reducing the thickness *d* for a given sampling fraction. Evidence for the validity of equation (3) is given in Fig. 3 (taken from [1]). The top plot shows energy resolution as a function of the sampling fraction for different sampling calorimeters using scintillating plate readout, with different absorbers. It is evident that energy resolution is indeed roughly inversely proportional to the square root of the sampling fraction. The bottom part of Fig. 3 shows data for fiber calorimeters. Again the energy resolution is inversely proportional to the square root of the sampling fraction and for a given sampling fraction it improves when thinner fibers are used. For example, for both calorimeters having a lead to plastic ratio of 4:1, the one with 0.5 mm fibers has an energy resolution about √2 times better than the one with 1 mm fibers. The same data taken from [1] are shown in Fig. 4 with points added for the H1 and KLOE calorimeters. The energy resolution is plotted as a function of the variable $\sqrt{d}/F_s$. The top portion shows only fiber calorimeters and the bottom shows data for other types of sampling calorimeters. The sampling fractions used in Fig. 3 and Fig. 4 are the ones for minimum-ionizing particles, which are usually somewhat different from the ones for showers (e/mip ≠ 1).

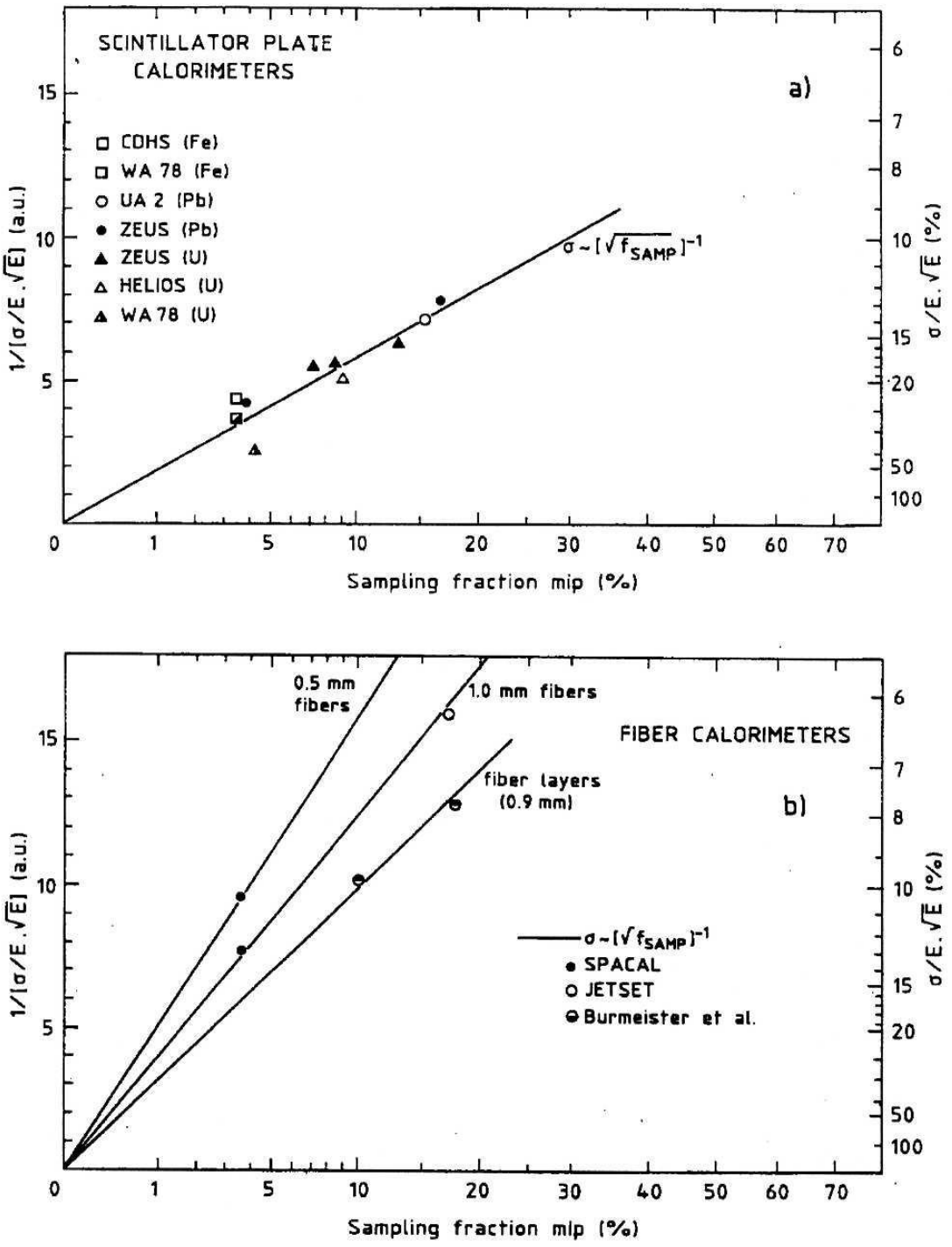

Fig. 3. (a) The EM energy resolution as a function of sampling fraction, for various representative plastic-scintillator plate calorimeters. (b) The same, for various fiber calorimeters (b). This figure taken from [1].

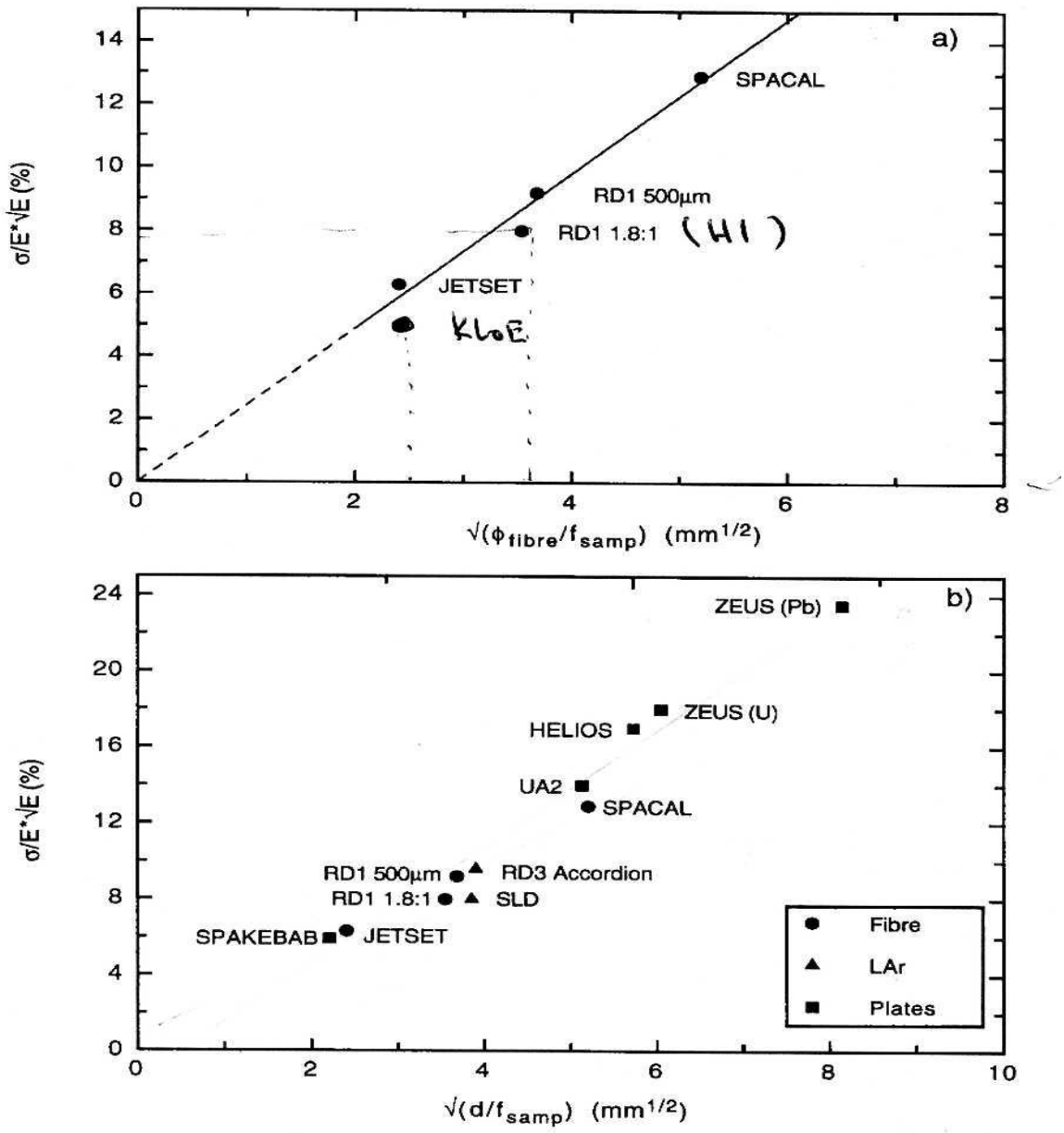

Fig. 4. Same data as on Fig. 3 plotted as a function of $\sqrt{d/F_S}$, where *d* is the thickness of the active media in mm (e.g. diameter of a fiber or thickness of a scintillator plate or liquid argon gap) and F_S is the sampling fraction for minimum ionizing particle in the calorimeter.

As discussed in [1], improvement of the EM energy resolution through an increased sampling fraction has its limits. Some of these are purely practical. Working with increasingly thinner fibers and absorber layers becomes rapidly very cumbersome. This is why we believe no one has used fibers thinner than 0.5 mm in diameter in full scale detectors. We will demonstrate that our technique is practically free from this limitation.

First, in Fig. 5 we briefly recall how the mechanical structures of fiber calorimeters were made in the past. Most operational detectors had monolithic towers or super-modules built by gluing. The gluing technique is simple and consists of piling lead sheets and fibers, applying a thin layer of optical epoxy to the top of each lead plate before the fibers are laid down and then to the fibers before the next plate is stacked. Each fiber is enveloped by glue in this way.

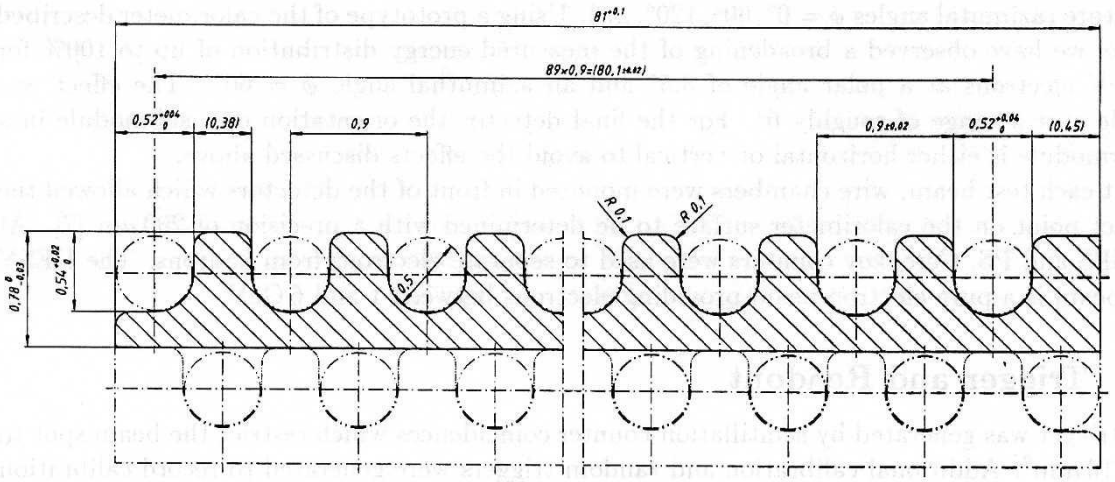

Front view of a lead plate with the grooves for 0.5 mm diameter scintillating fibres.

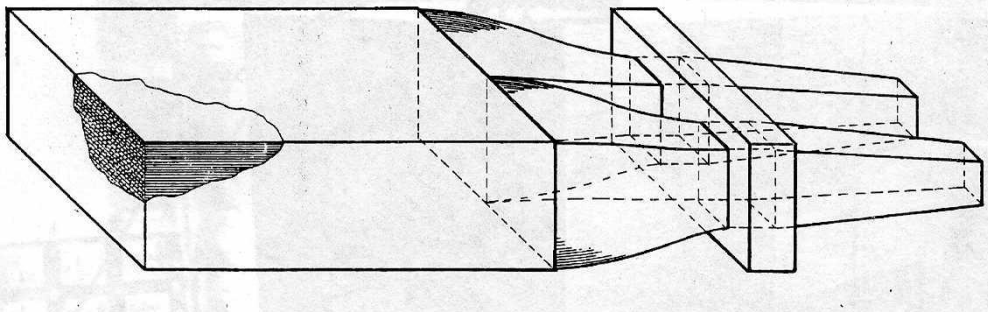

Schematic view of a submodule, the smallest detector unit.

Fig. 5. Schematic view of the typical mechanical structure of fiber calorimeters. A submodule and sampling structure of the H1 detector shown (picture taken from [3]).

Different R&D projects in the past employed various ways to construct calorimeter prototypes by simple piling without gluing, casting or brazing the absorber matrix, with fiber being inserted into channels afterward. Independent of which technique was used, their common weakness was extremely low level of possible automation of the assembly process. Essentially every single fiber or absorber layer had to be handled manually. This problem led to higher costs for fiber calorimeters compared to scintillation plate

detectors. This also limited sampling frequency because both thin absorber layers and thin fibers become difficult to handle. The other common characteristic of previous mechanical designs of fiber calorimeters is the placement of fibers inside the absorber volume. In particular, to our knowledge all detectors had fibers placed in straight lines parallel to each other in order to keep the sampling frequency within the tower volume constant. This is a direct consequence of construction of the absorber matrix from machined, rolled or extruded sheets.

A succinct description of our proposed technology is the following: We form a matrix of fibers and then the absorber is poured into this matrix. This makes it different from previous techniques, in the respect that every individual element of the calorimeter does not need to be handled separately.

We built two prototypes in 2003 and 2004 using tungsten powder as an absorber. The motivation at that time was pure conceptual, namely, to develop technology for compact calorimeters which could be used in compact detectors which have become feasible with the remarkable progress in micro pattern detectors.

Since a key element in our technique is utilization of W powder as an absorber we will list its properties first. The properties of tungsten powder as listed by the vendor are: particle size distribution 90% between 40 and 150 microns, bulk density 18.5 g/cm^3, tap density 11.25 g/cm^3, chemical composition W > 99.3%, Fe < 0.05%, Ni<0.05%, O_2<0.5%, others (Co, Cr, Mo, Cu) < 0.5%. This powder has very good fluidity for our applications.

Our first prototype had 16 towers. The towers were composed of W powder and square 0.25 mm x 0.25 mm BCF-12 scintillation fibers. There are 496 fibers per tower with the spacing between the fibers of 1 mm center-to-center in a staggered pattern. Dimensions for the tower active volume are 22 x 22 x 120 mm^3. The final density for different towers was slightly different, but for most of them was about 10.25 g/cm^3. The slight variation in final density was due to slightly different methods we used to pour W powder into the fiber matrix. Taking the effective radius of the fibers as 0.28 mm and a sampling fraction for mips of 1.2%, the stochastic term for energy resolution according to equation (3) should be close to 13%. A photograph of one of the towers is presented in Fig. 6.

Fig. 6. Photograph of a single tower of our first prototype with internal structure drawn on the wall of the brass container (scale is in cm). On the right is a view from the photodetector side (not to scale).

The mechanical structure of the first prototype required a thin wall (thickness 125 micron) brass container to keep powder and fibers in place. The assembly process can be described this way. First,

fibers were cut to ~ 15 cm length, then one tip of the fiber was slightly melted to form a small drop which worked as a stopper to prevent the fiber from slipping through the opening in the mesh. A stack of two meshes was then populated with fibers by undergraduate students. The lower mesh was fixed at the end of the brass container and this end of assembly was dipped into optical epoxy. Once the epoxy cured we prepared a container ready to be filled with W powder. The second mesh was kept floating. Tungsten powder was poured into the container from the top and at the same time this second mesh was pulled to the top. Powder flowed thruough the openings between the walls of mesh holes and fibers and filled the space on the bottom of the container, at the same time fixing fibers on place. During the filling process, the whole assembly was sitting on a vibrating platform. At the end of the process a small delrin cap with openings for the fibers was used to close the container. Fibers were epoxied inside this opening. The small diameter of the fibers makes them very flexible, with very little space needed to form a bundle of fibers at the end of the tower as seen in Fig. 6. The final steps were to machine both ends of the container and to glue a front face mirror (black block at position 0 cm in Fig. 6) in the front and a light guide at the back of the tower. With this technique, very compact assemblies can be made, but as we learned during a later test run, this method has significant flaws and we had to change the technique.

The first prototype matrix 4x4 towers was tested at the SLAC FFTB test line in 2003. The photodetectors we used were Hamamatsu R7400U mesh photomultipliers with additional external amplifiers and S8664-55 APDs operated at a gain of 50. A photograph of the test setup is presented in Fig. 7.

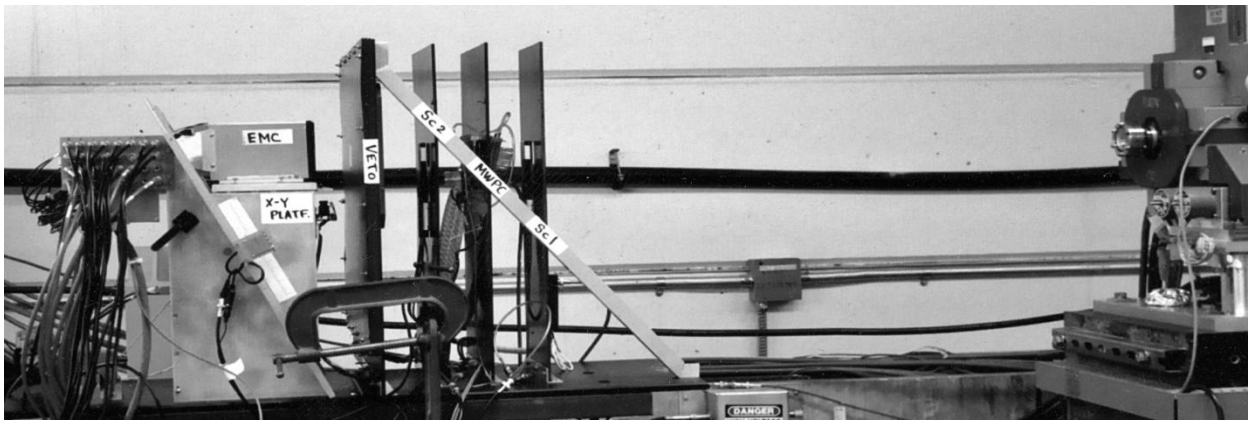

Fig. 7. Beam test setup at SLAC FFTB line. A coincidence between scintillation counters Sc1 and Sc2 provided the trigger. A Large veto counter with a hole in the middle and Pb converter were used to suppress background. Two small MWPCs provided XY coordinates to determine the impact point. The EMC was positioned on a 2D movable platform.

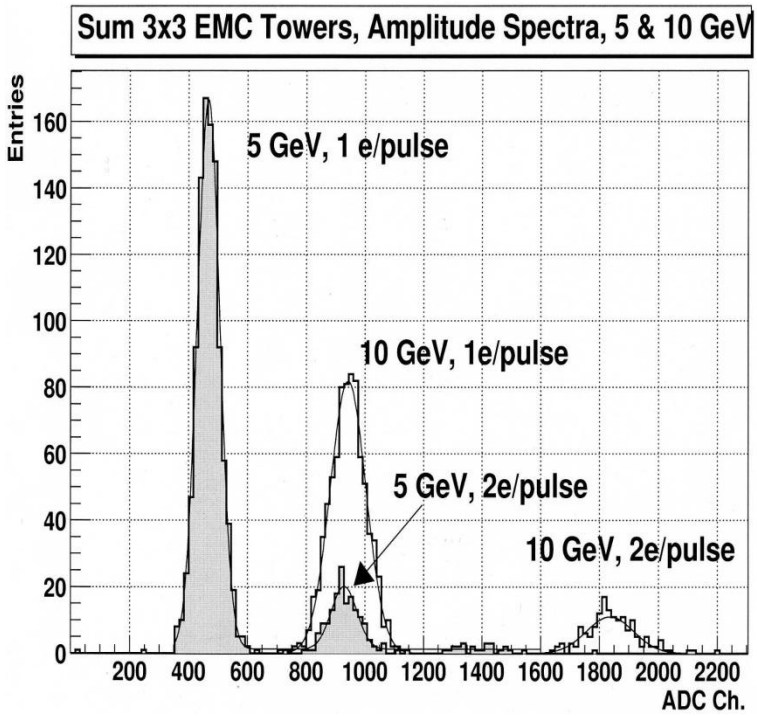

During calibration of the individual towers, we found that the observed energy resolution was not what we expected to see. The most striking observation was variation of a factor of two for the energy sum of a 3x3 tower cluster during the transversal scan of the matrix. Most of the 36 hours beam time allotted for the test was spent for different type of scans of the matrix both in the transverse and longitudinal directions. The results are summarized in the plot below. The best energy resolution for a single tower with impact point at the tower center was determined to be 17%/√E.

Fig. 8 Energy distribution for 3x3 sum of amplitudes during SLAC test run for Prototype 1.

The origin of large transverse non-uniformities was understood. The major contributing factors are dead layers near the tower edges and missing fibers in the tower corners (instead of 500 fibers we were left with 496 as four fibers one in each corner of the tower were removed to allow strings to pull the second mesh during filling). The non-uniformities observed during the longitudinal scans of the towers (+-10% maximum along the tower) were not well understood. The largest variations of response were observed for points located from 4 to 9 X_0 radiation lengths along the towers. One plausible explanation was that during packing process and recompression during stacking the array, the brass container might have undergone a slight distortion in the centers which led to a decreased sampling fraction in this region. There is also an indication that the cladding light might not be properly suppressed. Another factor that might have contributed to the non-uniform response is a light guide at the end of the tower which was not optimized prior to the test run. As we realized post factum, problems with non-uniformities were observed by many other groups and well described in [1]. Dense calorimeters will require very strict mechanical tolerances and a very uniform internal structure to achieve uniform response across the detector. A good example in this respect is the H1 electromagnetic calorimeter where tight mechanical tolerances were required during sub-module construction and final assembly of the detector.

To solve the problems with our first prototype we developed another method of combining powder and fibers. First we learned how to infuse optical epoxy into packed powder. A vacuum-assist method allows infusion of BC600 epoxy to a depth of 20 mm within 20 minutes. Epoxy has to be infused after packing because only dry powder has good fluidity. A few mechanical samples with a density of ~10.55 +-0.05 g/cm^3 were examined for uniformity. Local density variations were found to be within 2%. To

keep sampling frequency uniform along and across the tower we added additional intermediate meshes. These additional meshes allows arrangement of fibers in an accordion configuration, thus we got a “spacardion” structure. Since the whole assembly becomes rigid and stable there is no need for any type of external container. This eliminated dead material in the tower assembly. A single molding form was used to produce all subassembly units, which assured good mechanical tolerances and uniform sampling frequency between the towers. This time we used fibers with a diameter of 0.33 mm to match the openings in available standard perforated meshes. The distance between the fiber centers is 0.88 mm. Photographs of the mechanical prototype structures (with the square fibers left over from the first prototype) are shown in Fig. 9.

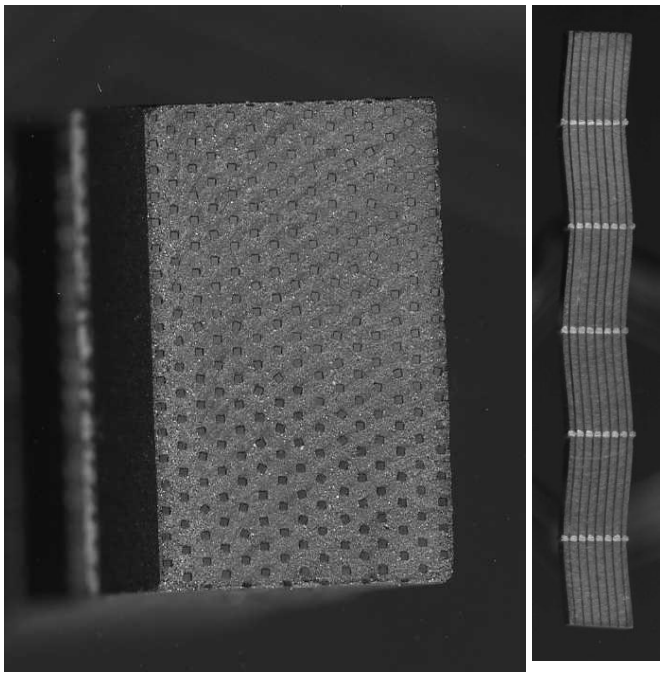

Fig. 9. Front and top view of the cross sections of the mechanical prototype. The distance between fiber centers is 0.88 mm. The fibers are placed in an accordion geometry.

For the second prototype every tower was glued from two sub-assemblies with the structure shown in Fig. 9. The reason for this is the stiffness of 345 fibers in a single subassembly unit, e.g. it was difficult to arrange 670 fibers in accordion shape at the same time. We believe that there multiple advantages for arranging fibers in an accordion type structure compared to the standard technique. First, all angular dependences should be significantly reduced. In particular, there is no way that a showering particle can cross the detector along the fiber (channeling effect for fiber calorimeters). Second, for a given amount of fibers, both the effective sampling frequency and sampling fraction are increased. Third, the number of fibers which contribute to the signal is increased, thus resolution degradation due to non uniformities in the response of a single fiber also should be reduced. We believe that with conventional construction techniques for fiber calorimeters, to create "spacardeon" structure would be almost impossible. Figure 10 below shows the cross section of mechanical tower built with this technique after gluing both sub-assembly units together.

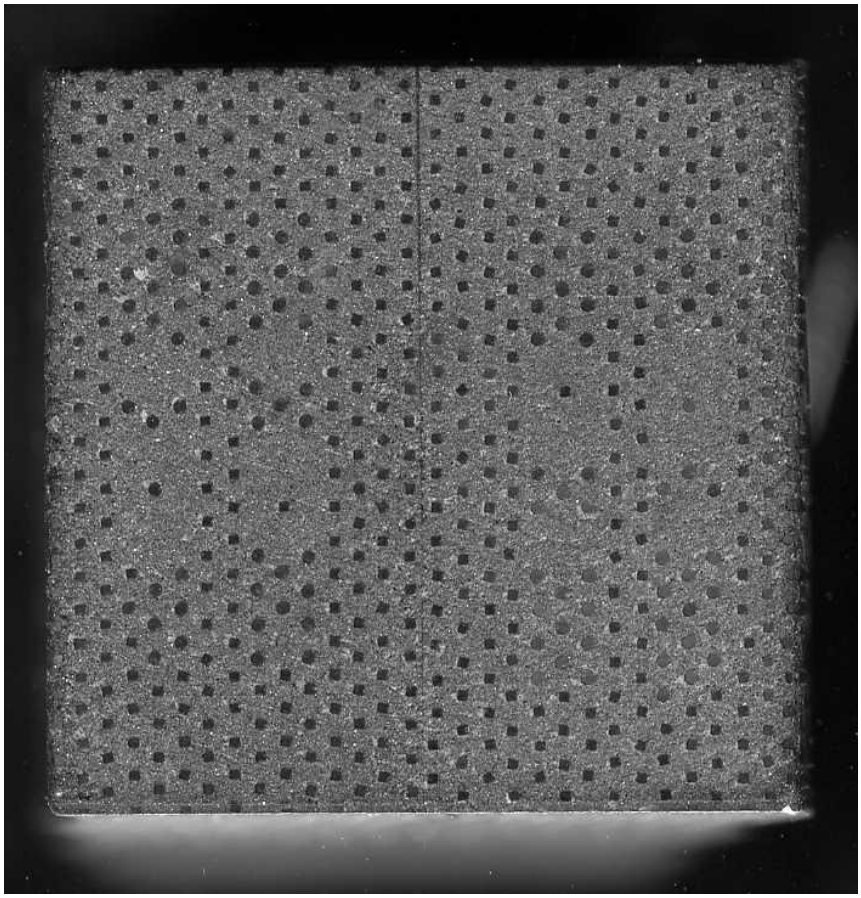

Good sampling uniformity is preserved right to the edges of the towers. This should solve problems with non-uniformities we experienced with our first device.

Fig. 10. Photograph of cross section of the mechanical prototype. The vertical line in the middle is a layer of glue which holds the two sub-assemblies together. The square fibers are 0.25 x 0.25 mm in dimension. For the mechanical prototype we didn't have enough fibers to fill all the holes, so we used a mixture of square and round fibers.

For our second EMC prototype we constructed a 3x4 matrix with the structure of towers as shown above. The size of this prototype was small, in order to learn how well this technique would work. Strict constraints on time, budget and manpower did not allow us to construct large detector. The final assembly unit, before the PMT block was attached, is shown in Fig. 11.

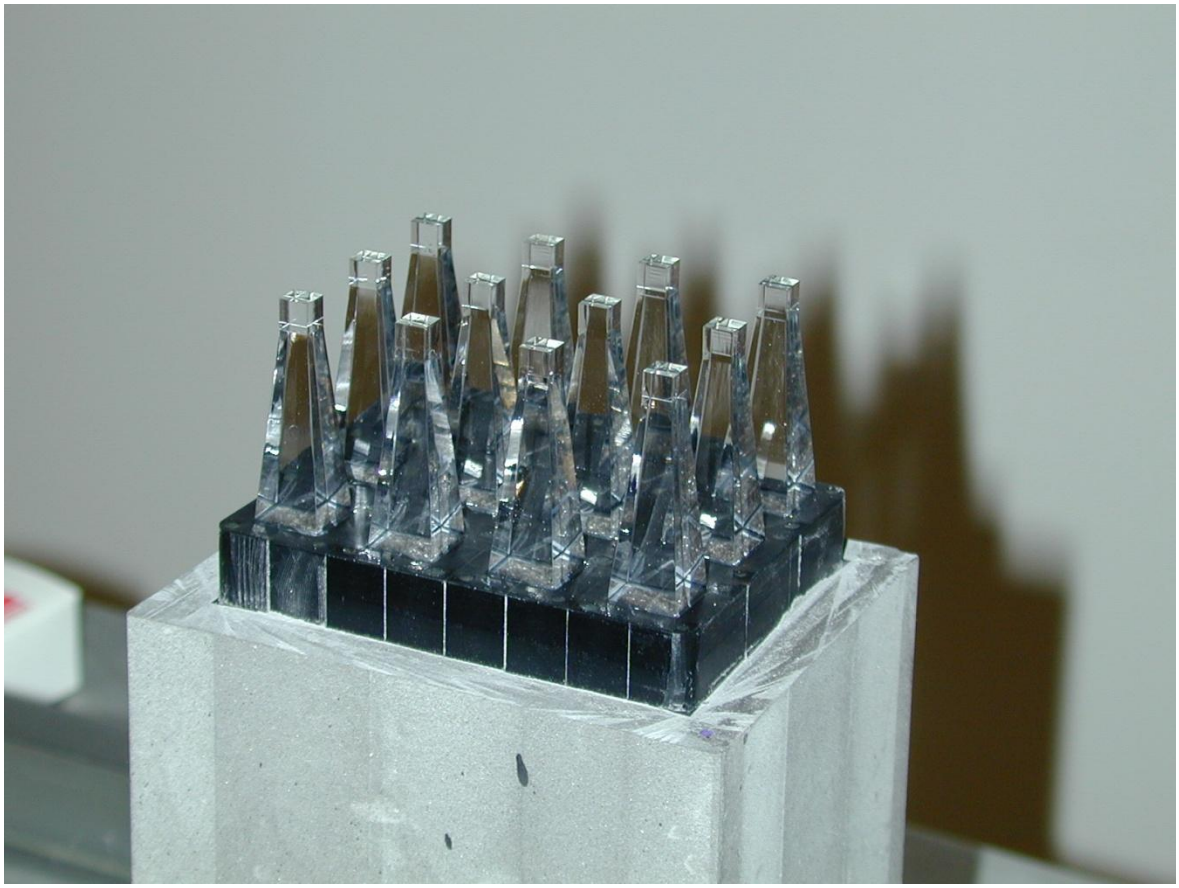

Fig. 11. Photograph of the final assembly. Black delrin blocks where fibers were bundled have the size of an active area. The gray external material is a mixture of W powder and epoxy to minimize edge effects for active towers.

Quite long and complicated light guides were required to achieve good uniformity of response across the surface of the tower with R5700U PMT readout. The size of the light guides at the end was chosen to be 4.9 x 4.9 mm^2 to allow readout with S8664-55 APDs as a second option. This reduced the cross section of the fiber bundle by about a factor of three.

This second prototype was scheduled for a test run at SLAC in the fall of 2004. The test run was first delayed and then SLAC was shut down due to an accident at the accelerator complex. We have not yet had an opportunity to test this prototype with a beam, thus, this method of building fiber calorimeters has yet to be proven.

To proof the principle we are proposing to build a larger prototype using techniques we developed for our second device. We will use the same structures (fibers/meshes) we used for our second device and the expected energy resolution should be close to 10%/√E. The radiation length and Molière radius will be about 0.7 cm and 1.8 cm. Ideally, we would like to use square fibers. There are three reasons why: better trapping efficiency for light, large surface area for the same sampling fraction compared

with cylindrical fibers and smaller output surface area because they pack much better. However, there are no available off-the-shelf perforated meshes with the desired dimensions. If we find appropriate meshes then we will use square fibers. We propose to expand the transverse tower size for this new prototype to about 2.8 x 2.8 cm^2. The length of the towers will be $20X_0$. We also would like to change slightly the method we used to construct the towers. For this third prototype we will build towers from four sub-tower units. We believe that a matrix of 6x6 towers would allow us to determine the efficiency of this technique with good confidence. With this matrix we also plan to get input information for possible continuing R&D for hadron calorimetry. In particular, one of the corner towers in the matrix may be constructed using non scintillating polystyrene fibers or fibers made of slow scintillator similar to BC 444. With this tower we can measure how much Cherenkov light we can detect and explore how well a dual read-out scheme would work.

If this technique works, (e.g. energy resolution, linearity and uniformity measured in the test run are good), then there are few other things which need to be investigated with this third prototype. The objectives are:

1. Investigate mechanical stability of the assembly; in particular, investigate how the parameters (optical, mechanical) of the towers will change under the mechanical load.
2. Investigate radiation hardness of the device, e.g. look at effects of radiation damage on scintillation fibers. Although good data exists in the literature [10] and general trends are known, in each case such studies have to be performed for the unique components of individual detectors. For us it would mean that after irradiation we would like to test this prototype with the beam one more time.

3. Application for Hadron Fiber Calorimeters.

If we will find that our technique works well for electromagnetic calorimeters we then will propose to do R&D for hadron calorimeters using the same technique. Applicability for both compensated and non-compensated dual readout devices can be investigated.

Apologists for fiber calorimetry technology like to compare the performance of the SPACAL calorimeter with the expected performance of two new detectors at LHC as shown below in Fig. 12 (from [11]).

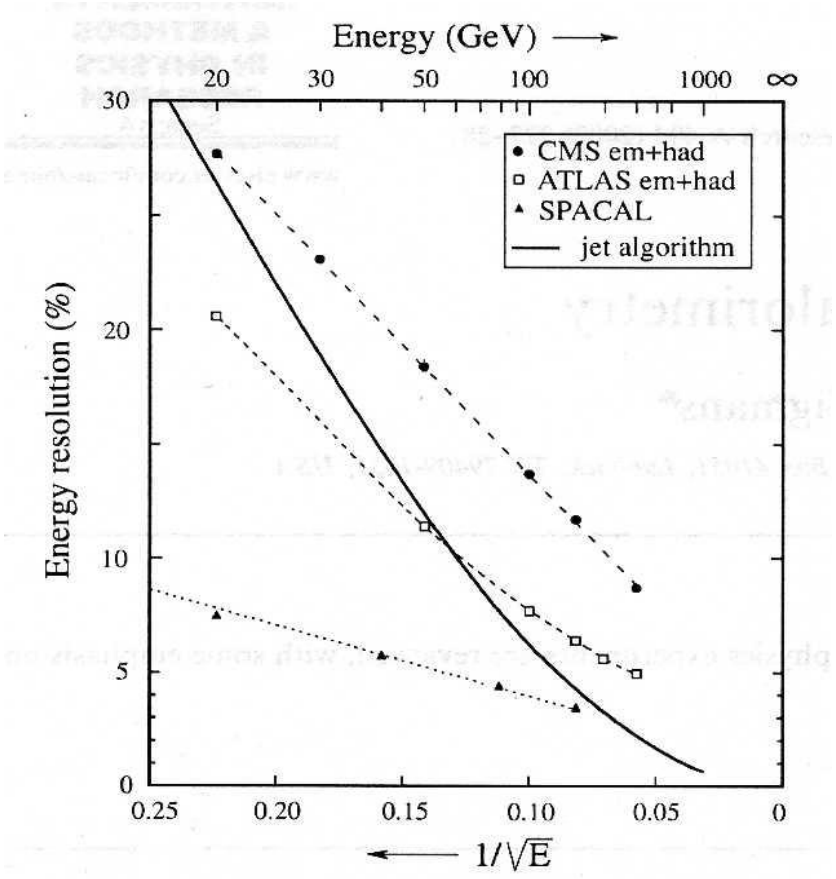

The point of showing the results this way is to illustrate that until recently, almost all calorimeter systems represent a compromise if one wants to measure both EM and hadronic showers. For example, the ZEUS collaboration operated a very-high-resolution hadron calorimeter, but paid a price in the form of rather mediocre performance for EM shower detection (18%/√E). This was a direct consequence of requiring compensation, which demands a small sampling fraction, which in turn leads to large sampling fluctuations. On the other hand, if one focuses on excellent EM resolution, one pays a heavy price when it comes to hadronic shower detection.

Fig. 12. The hadronic energy resolution of three calorimeter systems and the contribution of a jet-defining cone with R=0.3 to the jet energy resolution, as a function of energy.

As the author of [11] pointed out, once the choice is made for a crystal EM section (with a single readout technique), it essentially does not matter what you install behind it. The hadronic energy resolution will be poor. It will be completely determined by fluctuations in the energy sharing between

the EM and hadronic calorimeter sections, which have very different e/h values. Even the most sophisticated compensating hadronic section cannot alter this conclusion.

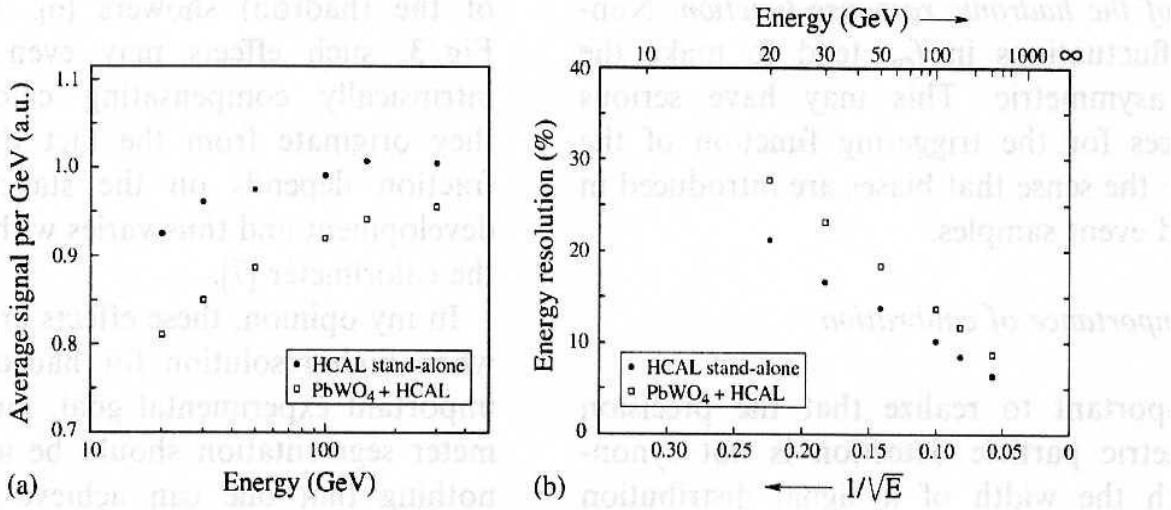

Fig. 13. Experimental results for pion detection in the prototype of the CMS calorimeter system. Shown are the response (a) and the energy resolution (b), as a function of the pion energy [11].

Fig 13 (a) shows the typical problems associated with non-compensated systems, which may in practice prove even more of a problem than the poor energy resolution [11]. Non-compensated calorimeters are intrinsically non-linear for hadrons, because of the energy dependence of the average EM shower fraction f_{em}. In the case of the CMS system, the large e/h value for crystals has the effect of deterioration of the hadronic signal linearity compared to stand-alone HCAL performance. Another adverse effect concerns the shape of the hadronic response function. Non-gaussian fluctuations in f_{em} tend to make the line shape asymmetric, which may have serious consequences for triggering. Calibration of non-compensated devices can be very tricky. As shown in [13] response of the calorimeter for high energy protons and pions may differ as much as 15%. Although for a known particle type one can make corrections, in the case of jets where the particle mix is unknown these corrections will be useless. The dual-readout technique potentially solves all the problems mentioned above. The proof of principle is presented in [12] where a calorimeter system with a dual readout EM section made of BGO crystals followed by a dual readout DREAM hadronic section provide excellent resolution for both EM and hadronic showers. But the price for such system will be very high. It should be pointed that this particular development of the dual-readout technique (BGO+DREAM) was specifically targeted for an ILC detector and for specific benchmark processes which require extremely good jet resolution from a calorimeter. This calorimeter system was optimized with other particular detector components (magnet, tracker etc.) for the specific physics processes to be studied.

The TESLA project [14] used a different approach to achieve excellent energy resolution for jets, usually referred to as the energy flow method (STAR is doing something similar for jet reconstruction using a TPC and barrel EMC with known limitations). The charge fragments of jets can be measured more precisely with the tracker than with calorimeter. However, calorimeter information is still needed

to account for contributions from neutral particles, mainly γs from π^0, but also K^0_S and neutrons. To do that properly a very high granularity calorimeter will be required. A high granularity allows recognition and elimination of all contributions from charge particles to the overall calorimeter signal. The remaining signal then can be assigned to the neutral components of the jet. For illustration Fig. 14, shows a SPACAL event display for a 150 GeV pion interacting with a thin target placed 1.5 m upstream.

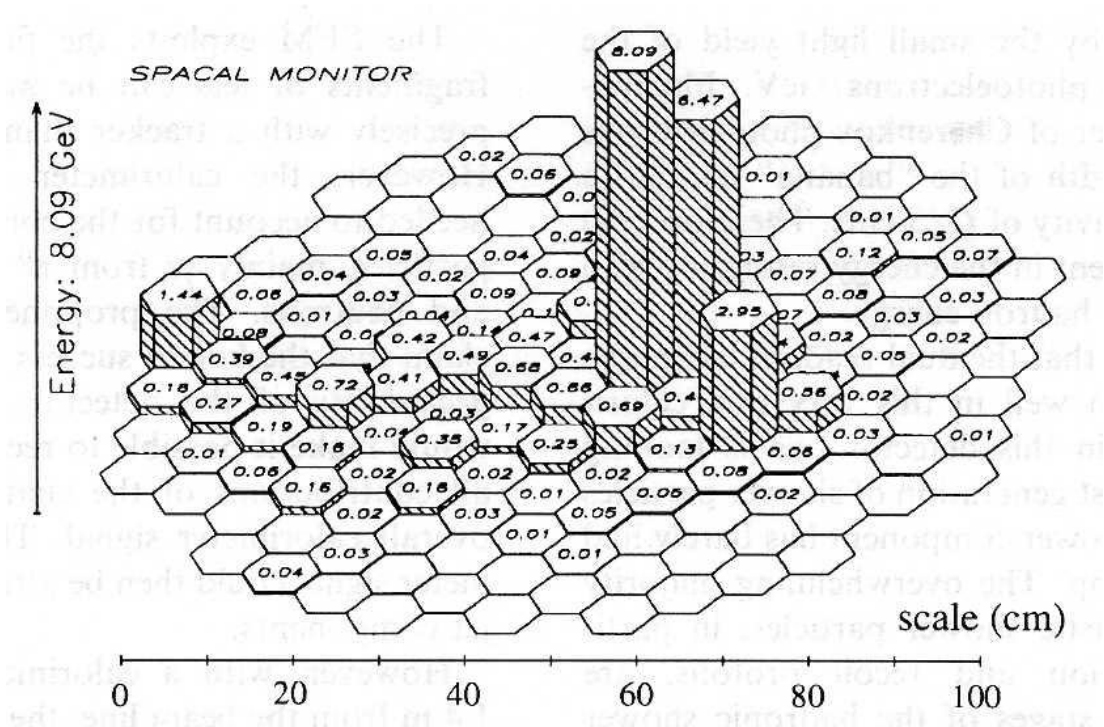

Fig. 14. A SPACAL event displays the reaction products from a 150 GeV pion interacted in an upstream target. The numbers denote the energy in (GeV) deposited in the individual calorimeter cells [15].

SPACAL was a very fine-grained calorimeter with the effective radius for each cell of 0.19 λ_{int} (2.0 R_M). Fig. 14 shows several individual reaction products that can be distinguished. However, there is also considerable overlap between the showers initiated by these particles. Smaller granularity will not help, since the size of the cell is already at the level when even electromagnetic showers will be spread among a few of them. For this reason, as proponents of SPACAL point out [11], the calorimeter system needs other qualities besides high granularity. In particular, it needs a good hadron energy resolution in order to measure jet energies with good precision. Again, we should mention that the discussion above should be viewed in the context of extremely strict requirements for jet measurements at an e^+e^- collider.

The previous rather long discussion was meant to convey that optimization of a hadron calorimeter or combined EM + hadron calorimeter system for an experiment is a challenging task. To be successful, it requires both well-established benchmark physics processes to be measured, and detailed knowledge of other detector and machine components (magnet, tracker, etc). For eRHIC this task is even more

complicated because of the broad range of colliding species which can be potentially studied. Thus, in our view, flexible calorimetry technology is very attractive for a particular detector optimization.

As we outline in our road map we would like to investigate two options. The first option is a compensated fiber calorimeter with good EM and hadronic energy resolutions and the second option, if feasible, a DREAM type device. To do that we will propose to build a compensated prototype with a tower size of about 6x6 cm^2 and length of ~5 λ_{int} If we find it feasible to measure electromagnetic fractions on an event-by-event basis after the first stage of R&D, then we probably will try to combine both compensated and DREAM type devices in a single prototype. One of the possible ways to do that is to use scintillating fibers made of slow scintillator (similar to BC 444). Figure 15 (taken from [16]) shows how separation of Cherenkov and scintillation light can be done for BGO crystals using digitization of the signal shape. The same principle probably can be applied to a fiber calorimeter. At this point we have not done a careful investigation of these options.

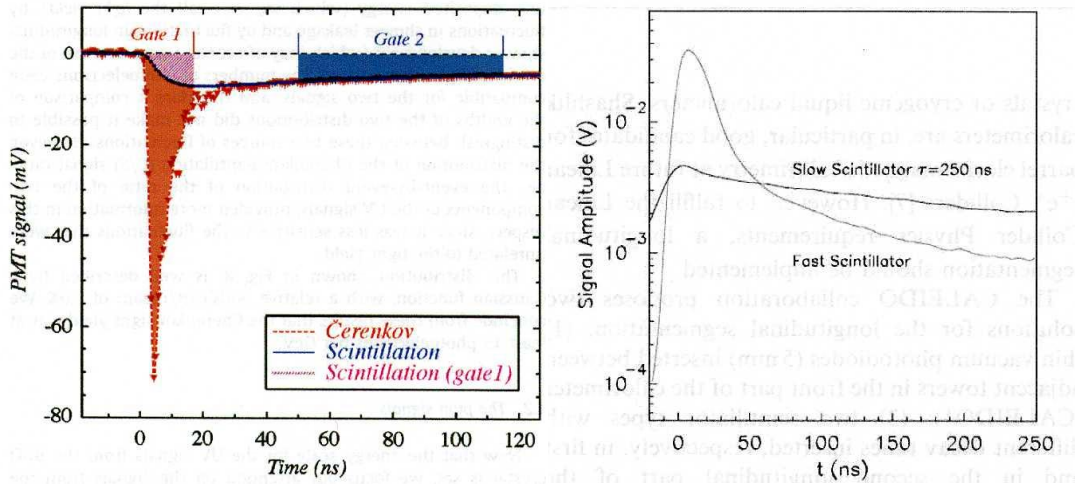

Fig. 15. Separation of scintillation and Cherenkov light in the BGO crystals (left). And timing structure of the CALEDO2 calorimeter prototype [17] with the first $5X_0$ of the detector made of BC 444 scintillator.

The major concern for a dual-readout technique is the number of Cherenkov photons per GeV which we can detect in our third prototype. It is quite possible that for showers of a few GeV range a dual readout technique may not work well because results will be limited primarily by photo-statistics.

The size of the hadronic prototype has to be significantly larger than the EM prototype, because for hadron calorimeters all sizes scale with λ_{int}. The longitudinal and radial containments $L_{95\%}$ and $R_{95\%}$ which are the required length and radius of the calorimeter for 95% hadronic energy deposition containment as given in [18] scales as:

$$L_{95\%} \approx t_{max} + 2.5\,\lambda_a, \quad R_{95\%} \approx 1\,\lambda_{int} \quad , \qquad (4)$$

where $t_{max} \approx 0.2\ln[E(GeV)] + 0.7$ is the shower maximum depth, and λ_a (in units of λ_{int}) describes the exponential decay of the cascade beyond t_{max} and varies with the energy as $\lambda_a = [E(GeV)]^{0.13}$. For our hadronic prototype the interaction length is about 18.5 cm. Taking equation (4) and assuming that the

initial test will be done at the AGS B2 test line (which is not operational at present) the required prototype would weigh about 1 ton. At this point we can not provide a more detailed description of the possible R&D program for hadron calorimetry as we believe it will evolve and our design will depend on experience gained by working with the EM prototype. However, the information listed above is sufficient for rough budget estimates.

4. Projective geometry.

Projective geometry in calorimetry always adds mechanical complication. For fiber calorimeters this has always been a big challenge and no easy solution has been found in the past. There have been only a few large projective prototypes (both EM and hadronic) built in the past. To keep the sampling fraction and frequency constant and a uniform response across the surface of the module, all of these previous examples used some sort of interleaved wedges as shown in Fig. 16 below (taken from ref. [1]).

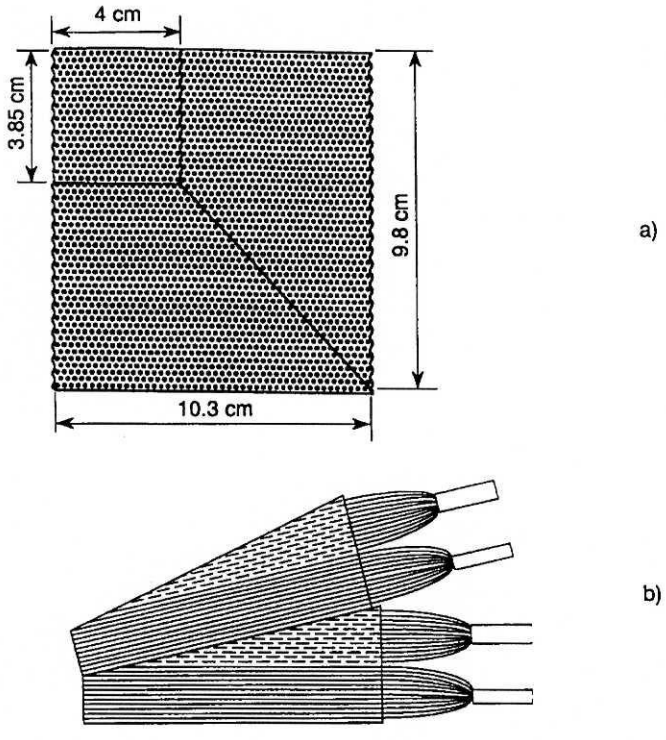

Fig. 16. The structure of the fully projective RD1 calorimeter. Shown are details of the front face of a tower (a) and a schematic (not to scale) of the longitudinal cross section of two neighboring modules (b).

If there is a strong requirement to build projective electromagnetic calorimeters for eRHIC (for the barrel it is probably required) and assuming that our technique works, then we will propose to investigate two methods to achieve projectivity with our technique and at the same time preserve simplicity of construction. The first possible approach is to use conical fibers, which preserve the sampling fraction along the trapezoidal tower, although not the sampling frequency. This will lead to some degradation of the energy resolution but will preserve the linearity of the detector. Conical

scintillation fibers to our knowledge are not available as an off-the-shelf product, but monofilament nylon line is. Since the process of producing both is probably similar, then it is quite possible that such fibers can be produced. The second approach that we can try is to increase the wiggling frequency along the tower. This seems possible for very thin fibers (similar to those we used for our first prototype, e.g. 0.25 mm x 0.25 mm). With proper tuning this will keep the sampling frequency and sampling fraction about the same, thus both linearity and energy resolution will be preserved. Because both techniques will require a lot of tuning and investigation we will postpone any significant effort to investigate these options until the first stages of the R&D program are completed.

5. BNL infrastructure.

We believe that all groups who will be doing R&D for eRHIC detectors will benefit from restoration of the B2 test line at the AGS. This beam line has a limited momentum range and rapidly diminishing fraction of electrons going from 0.5 to 7 GeV/c, but for our R&D program this is sufficient. Just as a side note, the STAR barrel EMC and BSMD still employ measurements from this test line during 1995-1998. In our budget request we allocated some funds to update our test beam setup. The equipment we used in 2003 at SLAC has to be significantly modified. Some of this equipment was specifically designed for SLAC FFTB beam line which has a quite narrow beam and slow repetition rate. The small active area of MWPCs and scintillation counters make them unusable at B2 test line at AGS. We are willing to share all test beam counters and scintillation hodoscopes build for our R&D with any other group who will be using B2 test line for their tests for eRHIC detectors. We believe that modules which are fully characterized by the test beam results greatly improve the quality of data taking in the final experiment. While it is impractical to test 100% of the calorimeter towers, a reasonable number of well tested towers embedded in the different locations in the final detector greatly speeds up the learning cycle in understanding data coming out of the detector. Thus we believe that investment for things like an operational test beam line at the AGS and common equipment for test beam experiments at BNL should be made.

6. Budget Proposal.

Based on quotes received so far, and using our prior experience, we have estimated the cost of the R&D for non-projective electromagnetic calorimetry in Table 3. We are planning to involve a significant number of UCLA undergraduate students to help us with the construction of the detectors.

A schedule for proposed first stage of R&D may look like this. Construction of the electromagnetic prototype will be during Jan. – Aug. 2010. Beam test sometime in between Nov. 2010 – Feb. 2011. This schedule is not rigid and mainly constrained by our involvement with STAR at RHIC.

Tungsten powder, sc. Fibers, epoxy and misc. mechanical components for 6x6 matrix	**$18k**
PMTs	**$20k**
Upgrade for DAQ and Test run equipment (electronics, test run counters, Sc. Hodoscope, cables etc.)	**$20k**
Machine Shop	**$15k**
Undergrad/Grad students labor	**$12k**
Shipping	**$10k**
Travel (5 people, 1 x 3 weeks)	**$15k**
Total for R&D Phase 1	***$110k***

Table 3. Cost breakdown for R&D Stage 1

REFERENCES:

1. Scintillating-fiber calorimetry, M. Livan, V. Vercesi, R. Wigmans . CERN Yellow Report, CERN-95-02
2. The DREAM Project –Results and plans, R. Wigmans, NIM A 572 (2007) 215-217
3. Performance of an Electromagnetic Lead/Scintillating-Fiber Calorimeter for the H1 Detector. H1 SPACAL GROU, DESY Red Report 95-165, NIM A374 (1996) 149-156
4. G. Drews et al., NIM A290 (1990) 335
5. E. Bernardi et al., NIM A262 (1987) 229
6. D. Acosta et al., NIM A308 (1991) 481
7. Quartz Fibers and the Prospect for Hadron Calorimetry at the 1% resolution level, R. Wigmans, Proceedings of the 7th International Conference on Calorimetry in HEP, Tucson 1997.
8. R. Wigmans, Calorimetry, Energy Measurement in Particle Physics, International Series of Monographs on Physics, Vol. 107, Oxford University Press, Oxford 2000.
9. R. Wigmans, NIM A259 (1987) 389
10. D. Acosta et al., NIM B62 (1991) 116-132
11. R. Wigmans, NIM A494 (2002) 277-287
12. N. Akchurin, et al, NIM A 598 (2009) 710-721
13. N. Akchurin, et al, NIM A 408 (1998) 380
14. TESLA Technical Design Report, Report DESY 2001-011, DESY, Hamburg, Germany, 2001
15. D. Acosta, et al., NIM A305 (1991) 55
16. 4th Letter of Intent. http://www.4thconcept.org/4LoI.pdf
17. A. C. Benvenuti et al., NIM A 461(2001) 373-375
18. C. Leroy and P. G. Rancoita, Rep. Prog. Phys. 63 (2000) 505-606